applied sciences

MDPI

Article

Experimental Investigation of the Concrete Cone Failure of Bonded Anchors at Room and High Temperature

Miora Nirina Robson [1,2,*], Omar Al-Mansouri [1], Nicolas Pinoteau [1], Marco Abate [3], Kenton McBride [3], Roberto Piccinin [3], Sébastien Rémond [2] and Dashnor Hoxha [2]

[1] Centre Scientifique et Technique du Bâtiment (CSTB), 84 Avenue Jean Jaurès, Champs-sur-Marne, CEDEX 2, 77447 Marne-la-Vallée, France; omar.almansouri@cstb.fr (O.A.-M.); nicolas.pinoteau@cstb.fr (N.P.)
[2] INSA CVL, LaMé, EA 7494, Univ Tours, Univ Orléans, 45100 Orléans, France; sebastien.remond@univ-orleans.fr (S.R.); dashnor.hoxha@univ-orleans.fr (D.H.)
[3] Hilti Corp., 9494 Schaan, Liechtenstein; marco.abate@hilti.com (M.A.); kenton.mcbride@hilti.com (K.M.); roberto.piccinin@hilti.com (R.P.)
* Correspondence: mioranirina.robson@cstb.fr

Abstract: Under fire conditions, bonded anchors often exhibit pull-out failure due to the thermal sensitivity of polymer-based adhesives. However, progress in manufacturing has allowed the development of more thermoresistant mortars, enhancing the probability of observing concrete-related failure modes at high temperature. For concrete cone failure, Annex D (Informative) to the European Standard EN 1992-4 provides a method to determine the characteristic fire resistance. This method is based on ISO 834-1 fire ratings and on limited experimental data without inclusion of bonded anchors. To remedy these shortcomings, the present contribution aims to provide the first experimental analyses on the concrete cone failure of bonded anchors loaded in tension and exposed to ISO 834-1 fire conditions, as well as heating with a relatively slower rate. The recorded ultimate loads show that the loss of capacity depends on the embedment depth, failure mode and heating scenario. Regarding exposure to ISO 834-1 fire, the 125 mm anchors lost 50% to 60% of their capacity at ambient temperature after 30 min to 75 min of fire exposure. The results highlight that the existing method gives a conservative prediction of the concrete cone capacity at high temperature. However, its accuracy can be improved. Moreover, the obtained crack patterns by the concrete cone breakout failure mode show that the rise in temperature did not significantly affect the geometry of the failure with slow-rate heating. In contrast, the ISO 834-1 fire conditions increased the radius of the failure cone at the exposed surface to up to 5.5 times the embedment depth. However, in any case, the initial slope of the failure surface was not significantly different from its value at ambient temperature.

Keywords: bonded anchors; concrete cone; high temperature; fire; experimental

check for updates

Citation: Robson, M.N.; Al-Mansouri, O.; Pinoteau, N.; Abate, M.; McBride, K.; Piccinin, R.; Rémond, S.; Hoxha, D. Experimental Investigation of the Concrete Cone Failure of Bonded Anchors at Room and High Temperature. *Appl. Sci.* **2022**, *12*, 4760. https://doi.org/10.3390/app12094760

Academic Editors: Aldina Santiago, Nicola Tondini and Luis Laim

Received: 24 March 2022
Accepted: 6 May 2022
Published: 9 May 2022

1. Introduction

In concrete structures, post-installed fastening techniques consist of using a steel rod to transfer external loads to hardened concrete via the contact between the two materials, which can be a mechanism of friction, mechanical interlock, bond or a combination of them [1]. Since they allow flexibility for the design of new concrete structures and the strengthening of existing ones, their use has increased in recent years. Among them, bonded anchors are a widely used technique, which consists of installing the steel rod in a drilled hole in hardened concrete and bonding it to the surrounding concrete with an adhesive mortar. The short-term and long-term behavior of bonded anchors has been the focus of several investigations [2–6], where it has been highlighted that this behavior is affected by different parameters such as installation conditions (drilling condition, hole cleaning, etc.) and in-service conditions (loading type, moisture, temperature, etc.). Moreover, the load-bearing capacity is directly dependent on the properties of the bonding material, which can be organic (with epoxy, polyester or vinylester), inorganic (cementitious, etc.) or a mixture of them [2,6]. When a bonded anchor located far from the edges of the concrete element and the neighboring anchors is loaded in tension, the three most frequent failure modes at ambient temperature are the pull-out failure, the concrete cone failure and the combined concrete cone and pull-out failure [5]. The pull-out failure corresponds to the debonding of the anchor over the whole embedment depth, which can occur at the concrete–mortar interface or at the mortar–steel interface. In general, the strength of this bond is specified for a given mortar after approval tests. The concrete cone failure is characterized by the extraction of a cone-shaped portion of concrete having its apex at the embedded end of the anchor, due to circumferential stresses. At ambient temperature, the slope of the failure surface is about 35° with respect to the horizontal plane [7], and the failure through an unstable crack propagation occurs when the cone-shaped crack that initiated at the embedded end reaches a critical length of about 45% of the slant height of the entire cone after a stable crack propagation phase [8].

Because fire represents one of the most severe environmental conditions to which structures may be subjected, the behavior of fasteners at high temperature is an important aspect of building design. In fact, they could experience a significant reduction in load capacity under fire, which must be taken into account for the holistic fire safety concept. Different investigations have been conducted around the qualification and design of fasteners under fire conditions. This problem often requires important efforts, as highlighted recently in a detailed discussion of the evaluation process to determine the fire resistance of anchor channels [9]. For post-installed anchors and rebars, a recent review presents the status of the regulations, as well as the underlying background [10]. Regarding bonded anchors, since the available bonding materials are mainly sensitive to temperature increases, the pull-out failure tends to be the most probable failure mode under high-temperature conditions. Different investigations have been devoted to the analysis of this resistance to pull-out failure at high temperature, in uncracked and cracked concrete [11–18]. However, the evolution of manufacturing technology has recently enabled the improvement of the fire resistance of adhesive mortars. Additionally, it is known that the mechanical strength of concrete can be substantially reduced with fire exposure [19]. Consequently, the probability to observe a concrete-related failure mode at high temperature, e.g., during an event of fire, is increased. For anchors in general, the concrete-related failure modes under fire conditions for both tension and shear loadings are not widely documented but are gaining interest. For example, a recent experimental and numerical study addressed the influences of concrete compressive strength, embedment depth and fire duration on the concrete pryout capacity of anchors [20].

Regarding the concrete cone failure, the resistance of cast-in-place and post-installed fasteners exposed to ISO 834-1 fire conditions can be determined with the method proposed in European Standard EN 1992-4 Annex D [21]. This method consists of decreasing the characteristic concrete cone capacity $N_{Rk,c}$ of a single anchor in cracked concrete at ambient temperature by a factor $k(t,h_{ef})$ depending on the exposure time t and the embedment depth h_{ef}, but independent of the type of anchor (Equation (1)):

$$\begin{gathered} N_{Rk,c,fi,(t)} = k(t,h_{ef})\cdot N_{Rk,c} \\ k(t,h_{ef}) = h_{ef}/200 \text{ for fire exposure up to 90 min} \\ k(t,h_{ef}) = 0.8\ h_{ef}/200 \text{ for 90 min } \leq \ t \ \leq \text{ 120 min} \end{gathered} \tag{1}$$

Even though Equation (1) applies for the design of bonded anchors, according to EN 1992-4 Annex D [21], no experimental evidence regarding the concrete cone capacity of bonded anchors during fire exposure has been reported in the literature. It is also worth noting that Equation (1) is supported by only a limited number of test results [22] and that, up to now, no additional experimental investigation on the concrete cone capacity of anchors during fire has been reported. This is because such tests require quite a complex setup and the results are difficult to predict. Alternatively, some recent studies investigated the residual concrete cone capacities of different post-installed anchors, i.e., the tests were performed after cooling down the concrete to ambient temperature [23–25].

The present contribution is therefore intended to address this need by analyzing the behavior of bonded anchors at high temperature without a cooling phase, with a focus on the concrete cone failure. Two types of heating scenarios are considered in this study: the standard ISO 834-1 fire and a less severe thermal load obtained with slow-rate heating. The detailed test program, setup and procedure are described, then the main test results are discussed.

2. Materials and Methods

2.1. Test Program and Test Specimens

The experimental campaign consisted of reference tests at ambient temperature and tests at high temperature, themselves subdivided into two groups according to the heating scenario: the slow-rate heating or the ISO 834-1 fire conditions. The experimental matrix is summarized in Table 1, where the symbol T refers to the high-temperature conditions. Two medium embedment depths were considered, 75 mm and 125 mm, which were chosen with regard to the probability of observing concrete cone failure, their practical significance and the technical constraints during the tests. In fact, shallower bonded anchors are more likely to fail by pull-out, and they are also of minor importance due to their limited capacity. On the other hand, deeper anchors are less sensitive to concrete damage after any reasonable exposure time. With the slow-rate heating, the four anchors were tested under similar thermal conditions, while with the ISO 834-1 fire, different levels of heating (30 min, 60 min and 75 min of exposure) were targeted for a similar embedment depth of 125 mm.

Table 1. Matrix of the test program.

Embedment Depth	75 mm	125 mm	Dimensions of Concrete Specimens
Ambient temperature	75-1 75-2 75-3 75-4	125-1 125-2 125-3 125-4 125-5	All anchors are installed in a common slab L 2.5 m × W 1.4 m × T 0.4 m
Slow-rate heating	T75-1 T75-2	T125-1 T125-2	Each anchor is installed in an individual slab L 1.5 m × W 0.5 m × T 0.4 m
Fire ISO 834-1	-	T125-ISO-30 T125-ISO-60 T125-ISO-75	Each anchor is installed in an individual slab L 1.5 m × W 0.65 m × T 0.4 m

Moreover, additional specimens were cast to determine the mechanical properties of concrete at ambient temperature at the time of testing. These consisted of cubes with sides of 150 mm to determine the compressive strength of the concrete according to NF EN 12390-3 [26], cylinders of 160 mm in diameter and 320 mm in height to determine the splitting tensile strength according to NF EN 12390-6 [27] and the modulus of elasticity according to NF EN 12390-13 [28]. Moreover, 600 mm long, 150 mm wide and 150 mm thick prisms were dedicated to three-point bending tests to determine the fracture energy of concrete according to RILEM TC 162-TDF 2002 [29].

The tested anchors consisted of carbon steel threaded rods installed in the hardened concrete slabs 36 days after their pouring. The bonding material consisted of an inorganic adhesive mortar, for which the installation procedure and curing time were specified by the manufacturer. The bond resistance of the adhesive mortar at ambient temperature was also determined experimentally according to the relevant approval test procedure [30], in the same concrete batch and with the same embedment depths, on the basis of three tests per embedment depth. The characteristics and mechanical properties at ambient temperature of the different materials constituting the anchoring system are listed in Table 2.

For the high-temperature tests, two thermocouple scales were installed inside each test specimen (Figure 1). The first was carried by a thin steel rod 3 mm in diameter, positioned perpendicularly to the exposed surface, to measure the temperatures of concrete at different depths along the thickness of the slab. The second was carried by a non-loaded witness anchor, which had exactly the same characteristics as the loaded anchor. The only difference is that for the witness anchor, the hole drilled in the concrete crosses the entire thickness of the slab to bring out the thermocouples through the unexposed face. It measured the temperatures at the concrete–steel interface, i.e., the temperatures of the adhesive mortar along the embedment depth. The positions of the thermocouples were chosen with respect to two fundamental conditions: they did not have to intercept the theoretical concrete cone, and they had to be far enough from the specimen edges to avoid any possible edge effects on the temperature distribution.

Table 2. Characteristics of the materials.

Threaded rod	Exterior diameter	16 mm
	Threads	2 mm
	Steel strength class	12.9
Adhesive mortar	Mean bond resistance	27 MPa
Concrete	Aggregate size	4 mm–10 mm
	Cement quantity	286 kg/m^3
	Water/cement ratio	0.54
	Cube compressive strength f_{cc}	33.6 MPa
	Tensile strength f_t	2.8 MPa
	Fracture energy G_F	71 J/m^2
	Young's modulus E	26.9 GPa

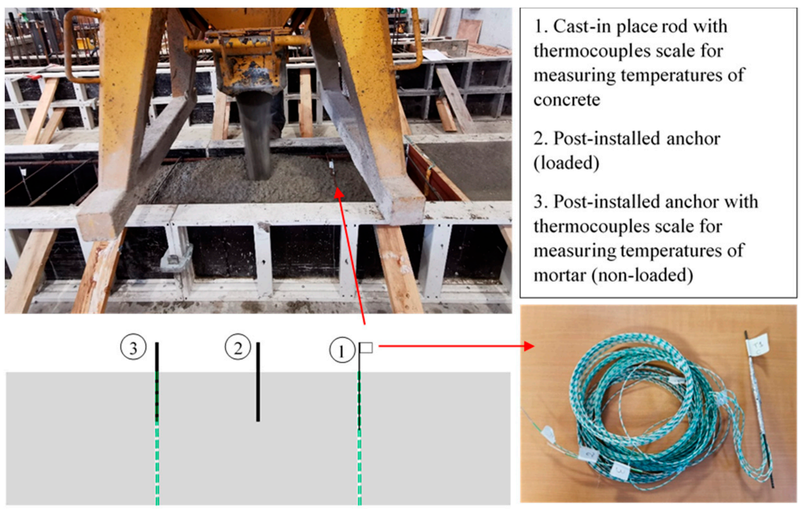

Figure 1. Positions of the thermocouples.

2.2. Test Procedures

The ambient temperature tests were performed following the standard unconfined tension test setup for technical approvals, specified in TR 048 [30]. The loading setup consisted of a displacement-controlled system, which allowed capturing the post-peak behavior of the anchor. A hydraulic jack transferred the load to the anchor through a high-strength steel rod, which was connected to a hollow cylinder cage, itself connected to the free end of the anchor by two coupling nuts. To prevent the vertical movement of the slab, the jack was supported by a steel ring, which rested directly on the slab. The dimension of the support was chosen sufficiently large, i.e., the diameter was larger than $4 \times h_{ef}$ to allow the formation of an unrestricted cone. The applied load was measured by a load cell placed on the top of the load cylinder. For measuring the anchor displacement, a linear variable differential transformer (LVDT) was installed on the top of the anchor in such a way that its axis and that of the anchor coincided.

For the slow-rate heating tests, the procedure consisted of two steps: the entire surface of the slab including the anchor was first heated with an electric heater, then after 3 h 30 min of exposure, the heater was removed, and a standard unconfined tension test was performed. Five to ten minutes were needed after the end of the heating to install the tension test setup, then the failure occurred 1 min to 3 min after the beginning of the test. Figure 2 shows the typical test setup for the tension tests at ambient temperature and for tests at high temperature after removing the electric heater.

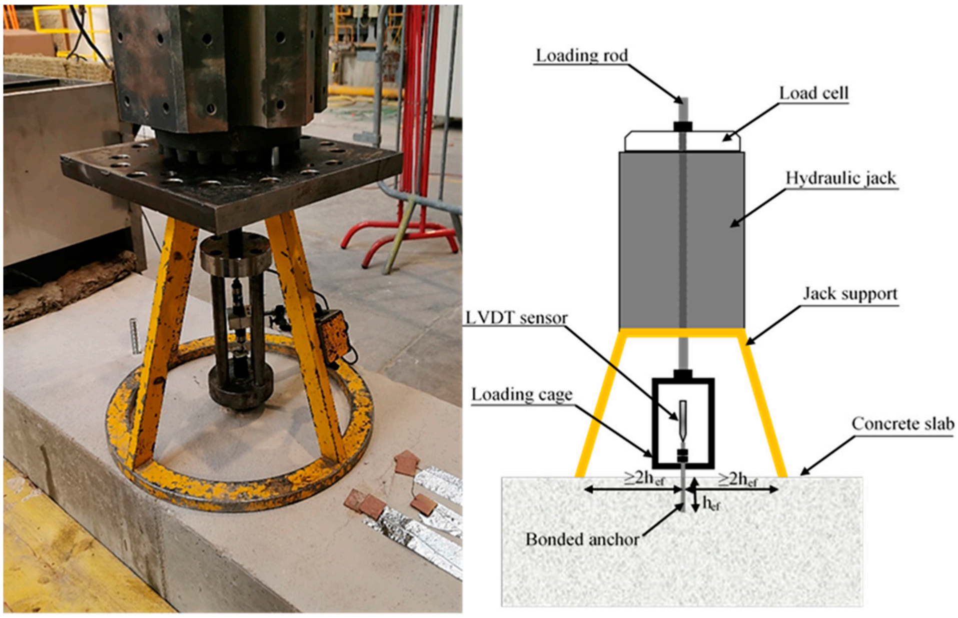

Figure 2. Test setup for tension tests at ambient temperature and after slow-rate heating.

For the tests with ISO 834-1 fire conditions, the thermal loading was ensured by a gas furnace, which heated the test specimen placed above the fire (Figure 3). Therefore, the slab was positioned upside down. The furnace was surmounted by a metallic frame, to which the mechanical loading equipment was directly fixed. The displacement imposed by the jack was transferred to the anchor via a rigid steel frame.

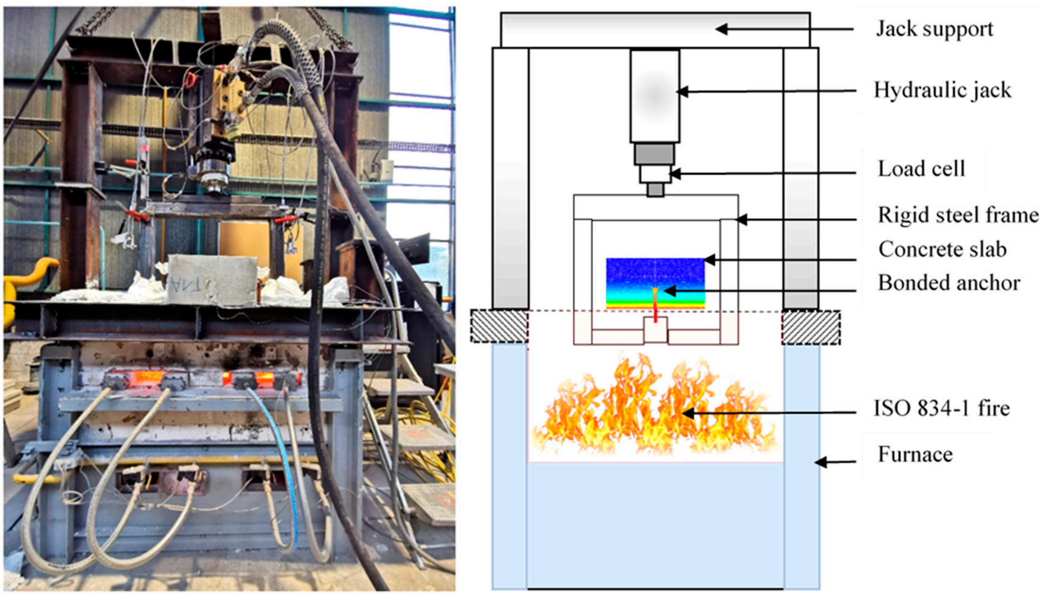

Figure 3. Setup for standard ISO 834-1 fire tests.

The first phase of the test consisted of heating the slab without applying a mechanical load. However, the self-weight of the rigid steel frame stressed the anchor permanently with a constant load of about 0.7 kN. The tests were performed exactly after 37 min (T125 ISO-30), 60 min (T125 ISO-60) and 75 min of exposure (T125 ISO-75) without stopping the heating. The failure occurred 3 min to 5 min after the beginning of the test, respectively, 40 min, 65 min and 78 min after the beginning of the heating.

3. Results

3.1. Temperatures Reached during the High-Temperature Tests

From the beginning of the heating, the thermocouples placed in the concrete and in the mortar recorded the temperatures at their positions. For comparison between the two heating scenarios, Figure 4 shows the typical evolution of the temperature of concrete measured by the thermocouples closest to the exposed surface, at a depth of 10 mm, for tests 75-1 (slow-rate heating) and T125-ISO-3 (ISO 834-1 fire conditions).

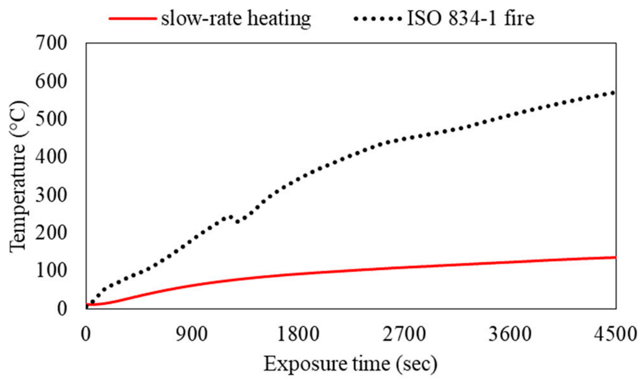

Figure 4. Evolution of the temperature of concrete at 10 mm from exposed surface.

The temperatures reached at different depths in concrete and in the mortar at the end of the slow-rate heating are presented in Figure 5. It is observed that at the same distance from the exposed surface, the temperature of the mortar was in general slightly higher than the temperature of concrete, but the thermal gradient was more pronounced in concrete. In concrete, the temperature at the exposed surface was about 225 °C, and the temperature at embedment depth was around 100 °C for 75 mm anchors and around 80 °C for 125 mm anchors. During the heating, the vapor flowed out freely through the non-exposed faces, and a through-thickness hole was made to bring out the thermocouples attached to the non-loaded witness anchor.

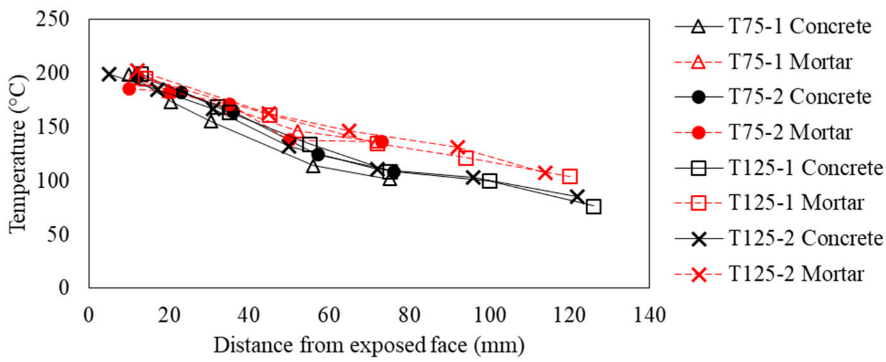

Figure 5. Thermal profiles in concrete and mortar at the end of the slow-rate heating.

For the tests conducted with ISO 834-1 fire conditions, the distribution of temperature in the concrete and in the mortar at the time of failure are presented in Figure 6. It can be observed that in the concrete, the thermal gradient was considerably more pronounced compared to the case of slow-rate heating. The temperature at the exposed surface was at least double that obtained with the slow-rate heating, while the temperature at the embedment depth did not exceed 50 °C, which is lower than that obtained with the slow-rate heating. Regarding the temperature of the mortar, the thermal gradient was less pronounced than in concrete; the temperature was lower than in concrete at the exposed face but higher at the embedment depth, where it was between 50 °C and 100° C. The water vapor also escaped through the lateral faces of the slab during the heating, and no spalling was observed.

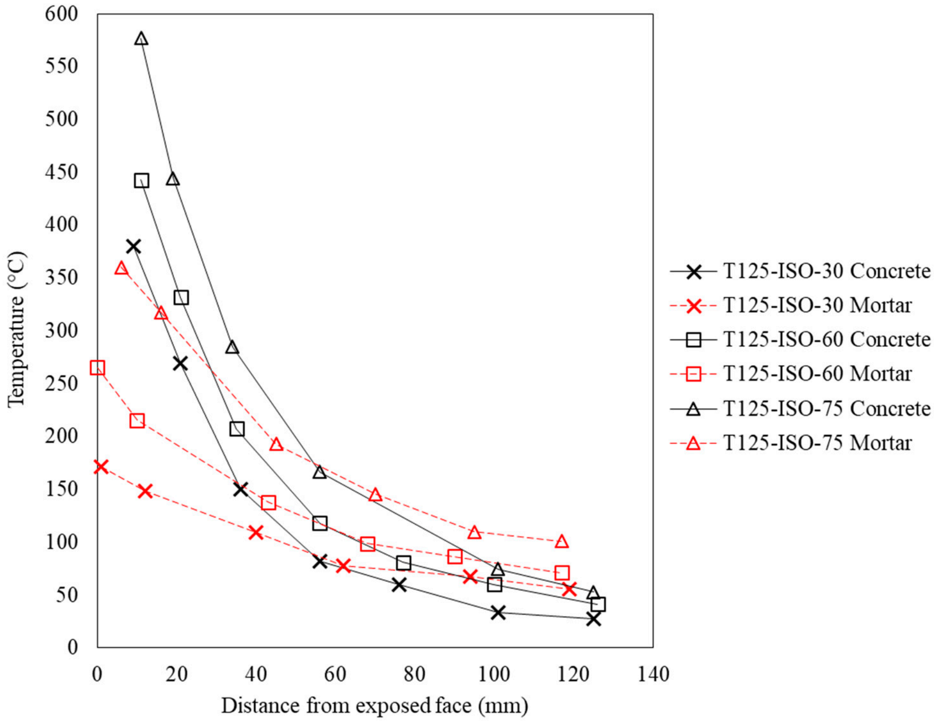

Figure 6. Thermal profiles in concrete and mortar with ISO 834-1 fire conditions.

3.2. Aspects of the Specimens after Testing

3.2.1. Failure Modes and Crack Patterns

For the tests at ambient temperature, the failure mode depended on the embedment depth: the 75 mm anchors experienced concrete cone failure, whereas the 125 mm experienced a combined concrete cone and pull-out failure at the concrete–mortar interface (Figure 7). This is coherent with the theory drawn from past observations that stipulates that the anchor fails by concrete cone failure when the embedment depth is between 3·d and 5·d (where d is the diameter of the anchor), whereas it fails by a mixed failure mode for greater embedment depths [1,3]. However, for the mixed failure mode, the height of the concrete cone part in past investigations was about 2·d to 3·d, while in the present study, it was 78 mm on average with a standard deviation of 12%, which corresponds to almost 5·d. Unfortunately, potentially key data that may explain this inconsistency, such as the fracture properties of concrete or the bond strength of the mortars, were not given in the past investigations. Moreover, the mechanism of combined failure is still subject to uncertainties, since theories differ on the question of which of the two mechanisms (debonding or concrete cracking) occurs first. The only known distinction that can be cited here is the nature of the mortar, which was organic (epoxy based) in the past investigations and inorganic in the present investigation.

For the tests with slow-rate heating, the typical crack patterns are presented in Figure 8. As can be seen, the anchors 75 mm deep underwent concrete cone failure, whereas the two anchors 125 mm deep (T125-1 and T125-2) experienced a combination of a concrete failure and pull-out failure. This difference suggests that the bond stress at the embedment depth exceeded the bond strength of the mortar for the 125 mm anchors, while it was not the case with the 75 mm anchors because the applied load was lower. In the T125-1 test, the concrete part was cone shaped with a height of 35 mm, while the rest of the anchors showed a pull-out failure at the concrete–mortar interface. Some radial cracks could be observed at the surface of concrete, but the specimen was not split. In the T125-2 test, the cone-shaped concrete part was not clearly observed, but instead, a horizontal crack crossed the slab in a plane parallel to the exposed face, at a depth of about 40 mm, and the layer of concrete thus formed was split into several portions after the peak load. The lower part of the anchor also underwent pull-out failure at the concrete–mortar interface.

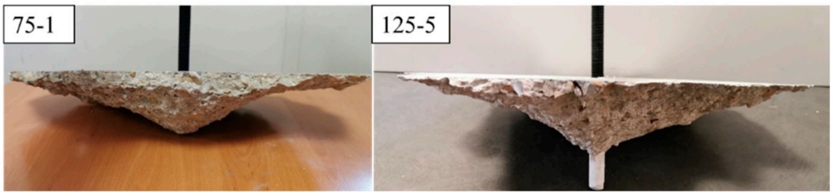

Figure 7. Typical crack patterns at ambient temperature.

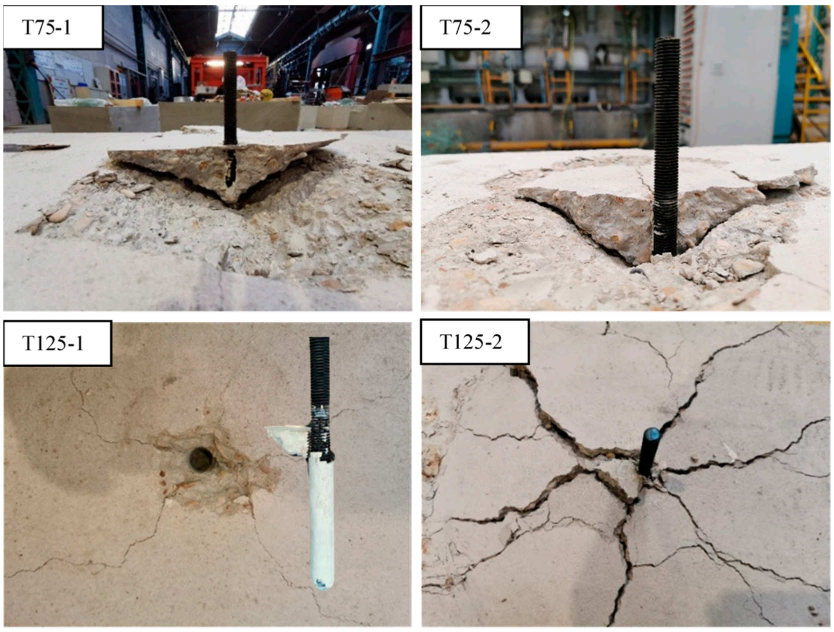

Figure 8. Crack patterns in slow-rate heating tests.

In the tests conducted with ISO 834-1 fire conditions, the crack patterns are shown in Figure 9. A clear concrete cone failure was obtained in the tests T125-ISO-30 and T125-ISO-60, whereas for T125-ISO-75, the crack pattern showed a combined failure, with a cone part over 60 mm of the depth and a debonding at the concrete–mortar interface over the remaining depth. It can be seen that in the case of clear concrete cone failure, the concrete cover was removed, leading to direct exposure of the rebar, which is particularly dangerous for a structure. It is also interesting to observe that T125-ISO-1 and T125-ISO-2 switched from a combined failure at ambient temperature to a pure concrete cone failure at high temperature. Knowing that at high temperature for those two anchors, the temperature of concrete near the embedded end was under 50 °C and did not exceed 100 °C at the mid-depth, one possible explanation for this change in failure mode is thus the contribution of the concrete near the exposed face, which was at considerably different temperatures under ambient conditions and under ISO 834-1 fire conditions.

A possible hypothesis is that cone-shaped cracks may initiate at different depths, and at ambient temperature, the crack that started at the embedded end was not fully developed (i.e., did not reach its critical length) before the debonding of the adhesive because the resistance of the concrete near the surface was sufficiently high. At high temperature, the concrete was severely heat damaged near the surface; therefore, it could not resist the unstable propagation of the cone-shaped crack initiated at the embedment depth while the bond strength of the mortar was not yet exceeded. Therefore, both the temperature of the mortar and the concrete along the whole depth are controlling parameters for the failure mode of bonded anchors, and the temperature of the concrete near the surface plays an important role, in particular.

Figure 9. Crack patterns in ISO 834-1 fire conditions tests.

3.2.2. Characteristics of the Concrete Cones

For the three test conditions, the slope of the concrete cone in the case of pure concrete cone failure varied around the circumference and along the crack path. The slope flattened when the crack reached the surface of the slab, as is particularly apparent in Figure 7 for ambient temperature, with T75-2 (Figure 8) and with T125-ISO-2 (Figure 9) for high temperature. Likewise, the horizontal extent of the cone at the surface was also variable. The minimum and maximum values of the failure angle β measured without considering the flattening part of the crack trajectory are presented in Table 3 for each test, together with the maximum radius r_{max} of the concrete cone measured at the surface. Those parameters are illustrated in Figure 10.

In the CCD method [7], it is considered that at ambient temperature, the horizontal extent of the failure surface is about three times the embedment depth, which corresponds to a radius of 1.5 h_{ef}. However, according to Table 3, the radius of the concrete cone could reach greater values, and it was particularly high in the tests with ISO 834-1 fire conditions, where the heat-damaged concrete cover 50 mm thick was removed over the entire exposed surface. Regarding the failure angle measured before the flattening of the crack path, its values seem not to be significantly affected by the temperature.

Table 3. Geometrical characteristics of the concrete cones.

Test Conditions	Test ID	h_{ef}	r_{max}	β
Ambient temperature	75-1	75 mm	2.8 h_{ef}	$17° \leq \beta \leq 22°$
	75-2	75 mm	3.2 h_{ef}	$17° \leq \beta \leq 28°$
	75-3	75 mm	2.5 h_{ef}	$16° \leq \beta \leq 25°$
	75-4	75 mm	1.8 h_{ef}	$28° \leq \beta \leq 39°$
Slow-rate heating	T75-1	75 mm	2.4 h_{ef}	$26° \leq \beta \leq 48°$
	T75-2	75 mm	2.1 h_{ef}	$22° \leq \beta \leq 27°$
ISO 834-1 fire conditions	T125-ISO-30	125 mm	5.2 h_{ef}	$19° \leq \beta \leq 34°$
	T125-ISO-60	125 mm	5.5 h_{ef}	$20° \leq \beta \leq 44°$

Figure 10. Failure angle and maximum radius of the concrete cone.

Apart from the geometrical aspects, it was also observed in the high-temperature tests that near the exposed surface, the aggregates particles, which are limestone based, experienced the typical chemical discoloration of limestone [31] at the different ranges of temperature reached. While their natural color was light ochre yellow at ambient temperature, they turned reddish-brown in tests with slow-rate heating (250 °C–300 °C) and gray in tests with ISO 834-1 fire (600 °C–800 °C) (Figure 11).

Figure 11. Discoloration of the aggregate particles near the exposed surface.

Finally, it was noticed that in the ambient temperature tests, the cracks mainly run through the aggregates, whereas at high temperature, they mainly went through the interfacial transition zone between aggregates and the cement paste, which was severely heat damaged. Therefore, most of the aggregates remained intact and could be easily removed from their positions. This indicates that the crack path was more torturous at high temperature, which potentially implies a larger failure surface.

3.3. Load–Displacement Curves and Ultimate Capacities

In Figure 12, the load–displacement curves recorded during the tests at ambient temperature and in the tests with slow-rate heating are presented, except for 75-3, for which the displacement could not be measured correctly.

For the 75 mm anchors, which all experienced concrete cone failure, the load–displacement curves show a first linear phase more or less overlapping for all the tests, whether at room or high temperature. Then, at high temperature, this phase is followed by a second non-linear phase, where the slope of the load–displacement curve decreases. The behaviors of the two anchors were different in this non-linear phase, resulting in different displacements despite quite similar peak loads.

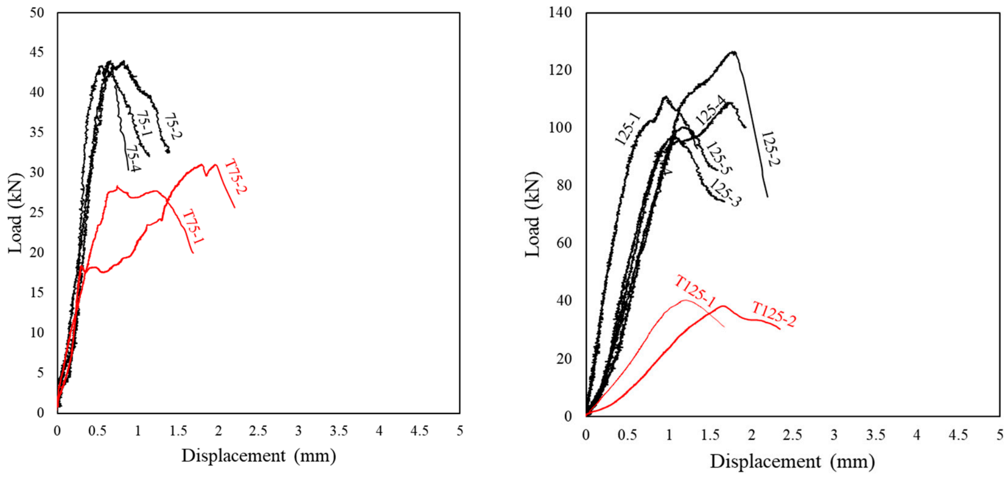

(**a**) (**b**)

Figure 12. Load–displacement curves for: (**a**) h_{ef} = 75 mm and (**b**) h_{ef} = 125 mm.

For the 125 mm anchors, which failed by combined failure, a first linear phase can also be seen in the load–displacement curves, where the curves are more or less superimposed for the tests at ambient temperature, except for 125-1. At high temperature, the curves have a less steep slope from the beginning of the tests, showing a more ductile behavior. The pre-peak branch does not appear to be clearly divided into linear and non-linear phases. Moreover, the post-peak phase shows a less abrupt decrease in capacity than at ambient temperature.

The ultimate capacities $F_{u,i}$ recorded in each of the tests are presented in Table 4, together with the loss of capacity due to fire, determined with reference to the mean ultimate capacity measured at ambient temperature, which was 43.2 kN for 75 mm anchors (concrete cone failure) and 108.7 kN for 125 mm anchors (combined failure). It is shown in Table 4 that the loss of capacity was greater for the 125 mm anchors than for the 75 mm anchors after a similar duration of exposure to slow-rate heating. This is because the combined failure of 125 mm anchors at high temperature combines a loss of capacity associated with the concrete cone part and a loss of capacity associated with the lowered bond strength of the mortar.

Regarding the four anchors that failed by the clear concrete cone (T75-1, T75-2, T125-ISO-30 and T125-ISO-60), the 125 mm anchors exposed to ISO 834-1 fire conditions lost a greater percentage of their capacities at room temperature, compared to the 75 mm anchors exposed to slow-rate heating despite a significantly shorter exposure time and despite the fact that the 75 mm anchors were entirely positioned in concrete at over 100 °C, while the 125 mm anchors were surrounded by concrete at under 100 °C over half of their depths. This supports the previous assertion that the temperature of the concrete near the surface of the slab is particularly important for the concrete cone capacity.

Finally, based on the capacity predicted by Equation (1) for the 125 mm anchor exposed to ISO 834-1 fire for up to 90 min, the test results confirm that this equation is conservative. However, as only one capacity applies between 0 min and 90 min of exposure based on an equation derived at 90 min, the safety level increases when the exposure time decreases. For the anchor that failed after 40 min of exposure (T125-ISO-30), the predicted capacity is almost half (55%) of the actual capacity of the anchor. Regarding the 75 mm anchors exposed to slow-rate heating, Equation (1) predicts in the case of ISO 934-1 fire a capacity of 8.39 kN for an exposure time up to 90 min and 6.71 kN for an exposure time between 90 min and 120 min. Those predictions are excessively conservative compared to the test results because they represent less than 30% of the actual capacities of the anchors. This highlights that Equation (1) is not appropriate when the heating scenario differs from ISO 834-1 fire conditions, hence the need for an alternative method.

Table 4. Ultimate loads and loss of capacity due to fire.

Test Condition	Test ID	Failure Mode	$F_{u,i}$ (kN)	Loss of Capacity	Equation (1)
Ambient temperature	75-1	Concrete cone	43.4		
	75-2	Concrete cone	44.0		
	75-3	Concrete cone	41.4		
	75-4	Concrete cone	44.0		
	125-1	Concrete cone + pull-out	111.0		
	125-2	Concrete cone + pull-out	126.5		
	125-3	Concrete cone + pull-out	96.9		
	125-4	Concrete cone + pull-out	108.8		
	125-5	Concrete cone + pull-out	100.3		
Slow-rate heating	T75-1	Concrete cone	31.1	28%	
	T75-2	Concrete cone	28.4	34%	
	T125-1	Concrete cone + pull-out	40.3	62%	
	T125-2	Concrete layer + pull-out	38.3	65%	
Fire ISO 834-1	T125-ISO-30	Concrete cone	54.7	50%	30.08
	T125-ISO-60	Concrete cone	46.2	57%	30.08
	T125-ISO-75	Concrete cone + pull-out	44.9	59%	30.08

4. Conclusions

In this experimental investigation, the behavior of single-bonded anchors with inorganic adhesive mortar subjected to a monotonic tensile loading under ambient and high-temperature conditions was studied considering two embedment depths: 75 mm and 125 mm. In addition to the ISO 834-1 fire, slow-rate heating was also considered to analyze the effect of different temperature conditions. One main specificity of this investigation is that the test setup allowed performing the tests at high temperature without a cooling phase. Four of the seven tests performed at high temperature resulted in a clear concrete cone failure. The ultimate load obtained in those tests broadens the existing database for the concrete cone capacity of anchors at high temperature, which does not currently include the capacity of bonded anchors.

The following main findings can be reported based on the experimental results:

- With the slow-rate heating, the temperature of the mortar was higher than that of concrete at a similar depth, but the thermal gradient along the whole depth was more pronounced in the concrete than in the mortar. For a similar exposure time, the 75 mm anchors experienced concrete cone failure, while the 125 mm anchors experienced a combined failure. Moreover, the loss of capacity due to the thermal load was more important for the 125 mm anchors, as it combined a loss of concrete cone capacity and a loss of bond strength of the mortar.
- With the ISO 834-1 fire conditions, considerably higher temperatures were reached in concrete at the exposed surface compared to the case with the slow-rate heating, but the thermal gradient was also more pronounced, hence the temperature of concrete at embedment depth was lower than with the slow-rate heating. When increasing exposure time, the failure mode of the 125 mm anchors changed from clear concrete cone failure to a combined failure.
- The analysis of temperature distributions suggests that not only the temperature of the mortar controls the change of failure mode between a clear concrete cone failure and a combined failure, but also the temperature of concrete over the entire embedment depth.
- In all tests, the slope of the cone-shaped failure surface varied along the crack path and around the circumference of the cone and flattened when reaching the surface of the slab. The temperature did not have a significant influence on this slope before the

flattening. However, in the tests with ISO 834-1 fire conditions, the base radius of the cone at the exposed surface reached up to 5.5·h_{ef}.

- The displacement of an anchor after thermal exposure is not predictable based on the present results because each anchor behaved differently after a linear load–displacement relationship at the beginning of the loading. This linear phase was not affected by the temperature in the case of concrete cone failure, while a more ductile behavior was in the case of combined failures.
- The comparison between the measured and predicted capacities based on the current method in EN 1992-4 Annex D shows that this latter is actually conservative for bonded anchors. However, its accuracy can be improved, especially for short exposure times. Finally, an alternative prediction method is necessary to cover the case of heating scenarios different from the standard ISO 834-1 fire.

Author Contributions: Conceptualization, M.N.R., O.A.-M. and N.P.; methodology, M.N.R., O.A.-M., N.P., M.A., K.M. and R.P.; formal analysis, M.N.R., O.A.-M., N.P., M.A., K.M., R.P., S.R. and D.H.; investigation, M.N.R.; resources, N.P., M.A., K.M. and R.P.; data curation, M.N.R.; writing—original draft preparation, M.N.R.; writing—review and editing, M.N.R., O.A.-M., N.P., M.A., K.M., R.P., S.R. and D.H.; visualization, M.N.R. supervision, S.R. and D.H.; project administration, N.P. and M.A.; funding acquisition, N.P. All authors have read and agreed to the published version of the manuscript.

Funding: This research received no external funding.

Institutional Review Board Statement: Not applicable.

Informed Consent Statement: Not applicable.

Data Availability Statement: Not applicable.

Acknowledgments: The research presented in this paper was conducted at Centre Scientifique et Technique du Bâtiment (CSTB). The authors would like to acknowledge the staff of the fire resistance laboratory of Stéphane Charuel at CSTB for their contribution to the experimental campaign.

Conflicts of Interest: The research presented in this paper was sponsored by Hilti AG and CSTB. The support of these organizations is gratefully acknowledged. The findings, opinions and conclusions are those of the authors and do not necessarily reflect those of the sponsoring organizations.

References

1. Eligehausen, R.; Mallée, R.; Silva, J.F. *Anchorage in Concrete Construction*; John Wiley & Sons: Hoboken, NJ, USA, 2006; ISBN 978-3-433-01143-0.
2. Cook, R.A.; Kunz, J.; Fuchs, W.; Konz, R.C. Behavior and Design of Single Adhesive Anchors under Tensile Load in Uncracked Concrete. *Struct. J.* **1998**, *95*, 9–26. [CrossRef]
3. Cook, R.A.; Doerr, G.T.; Klingner, R.E. Bond Stress Model for Design of Adhesive Anchors. *Struct. J.* **1993**, *90*, 514–524. [CrossRef]
4. Higgins, C.C.; Klingner, R.E. Effects of Environmental Exposure on the Performance of Cast-in-Place and Retrofit Anchors in Concrete. *Struct. J.* **1998**, *95*, 506–517. [CrossRef]
5. Eligehausen, R.; Cook, R.; Appl, J. Behavior and Design of Adhesive Bonded Anchors. *ACI Struct. J.* **2006**, *103*, 822–832. [CrossRef]
6. Fujikake, K.; Nakayama, J.; Sato, H.; Mindess, S.; Ishibashi, T. Chemically Bonded Anchors Subjected to Rapid Pullout Loading. *ACI Mater. J.* **2003**, *100*, 246–252.
7. Fuchs, W.; Eligehausen, R.; Breen, J.E. Concrete capacity design (CCD) approach for fastening to concrete. *ACI Struct. J.* **1995**, *92*, 73–94.
8. Eligehausen, R.; Sawade, G. *A Fracture Mechanics Based Description of the Pull-Out Behavior of Headed Studs Embedded in Concrete*; Chapman and Hall: London, UK, 1989; ISBN 0-412-30680-8.
9. Mahrenholtz, C.; Tian, K. Fire Rating of Anchor Channels and Channel Bolts. In Proceedings of the 2021 World Congress on Advances in Structural Engineering and Mechanics (ASEM21) GECE, Seoul, Korea, 23–26 August 2021.
10. Mahrenholtz, P.; Sharma, A. Fire Rating of Post-Installed Anchors and Rebars. *CivilEng* **2020**, *1*, 216–228. [CrossRef]
11. Pinoteau, N.; Pimienta, P.; Guillet, T.; Rivillon, P.; Rémond, S. Effect of heating rate on bond failure of rebars into concrete using polymer adhesives to simulate exposure to fire. *Int. J. Adhes. Adhes.* **2011**, *31*, 851–861. [CrossRef]
12. Pinoteau, N.; Heck, J.V.; Rivillon, P.; Avenel, R.; Pimienta, P.; Guillet, T.; Rémond, S. Prediction of failure of a cantilever–wall connection using post-installed rebars under thermal loading. *Eng. Struct.* **2013**, *56*, 1607–1619. [CrossRef]

13. Lahouar, M.A.; Caron, J.-F.; Pinoteau, N.; Forêt, G.; Benzarti, K. Mechanical behavior of adhesive anchors under high temperature exposure: Experimental investigation. *Int. J. Adhes. Adhes.* **2017**, *78*, 200–211. [CrossRef]
14. Lahouar, M.A.; Pinoteau, N.; Caron, J.-F.; Foret, G.; Rivillon, P. Fire design of post-installed bonded rebars: Full-scale validation test on a 2.94 × 2 × 0.15 m_3 concrete slab subjected to ISO 834-1 fire. *Eng. Struct.* **2018**, *174*, 81–94. [CrossRef]
15. Al-Mansouri, O.; Mege, R.; Pinoteau, N.; Guillet, T.; Rémond, S. Influence of testing conditions on thermal distribution and resulting load-bearing capacity of bonded anchors under fire. *Eng. Struct.* **2019**, *192*, 190–204. [CrossRef]
16. Al-Mansouri, O.; Mege, R.; Pinoteau, N.; Guillet, T.; McBride, K.; Abate, M.; Rémond, S. Design Recommendations for Bonded Anchors under Fire Conditions Using the Resistance Integration Method. *Appl. Sci.* **2021**, *11*, 7810. [CrossRef]
17. Lakhani, H.; Hofmann, J. A Numerical Method to Evaluate the Pull-Out Strength of Bonded Anchors under Fire. In Proceedings of the 3rd International Symposium on Connections between Steel and Concrete, Stuttgart, Germany, 27–29 September 2017; pp. 1179–1190.
18. Muciaccia, G.; Navarrete, D.D.; Pinoteau, N.; Mége, R. Effects of different test apparati and heating procedures on the bond properties of post-installed rebar connections under elevated temperatures. *Mater. Struct.* **2019**, *52*, 47. [CrossRef]
19. Schneider, U. Concrete at high temperatures—A general review. *Fire Saf. J.* **1988**, *13*, 55–68. [CrossRef]
20. Tian, K.; Ožbolt, J. Concrete pry-out failure of single headed stud anchors after fire exposure: Experimental and numerical study. *Eng. Struct.* **2021**, *232*, 111816. [CrossRef]
21. *NF EN 1992-4—Eurocode 2—Design of Concrete Structures—Part 4: Design of Fastenings for Use in Concrete*; CEN (European Comitte for Standarization): Brussels, Belgium, 2008.
22. Reick, M. Brandverhalten von Befestigungen mit großem Randabstand in Beton bei Zentrischer Zugbeanspruchung (Fire Resistance of Anchors Far from an Edge in Concrete with Axial Loading). Ph.D. Thesis, University of Stuttgart, Stuttgart, Germany, 2001.
23. Hlavička, V.; Lublóy, É. Concrete cone failure of bonded anchors in thermally damaged concrete. *Constr. Build. Mater.* **2018**, *171*, 588–597. [CrossRef]
24. Bamonte, P.; Gambarova, P.G.; Muciaccia, G. Ultimate Capacity of Undercut Fasteners Installed in Heat-Damaged Concrete. *J. Struct. Eng.* **2020**, *146*, 04020225. [CrossRef]
25. Sharma, A.; Bosnjak, J. Residual Tensile Capacity of Post-Installed Anchors after Exposure to Fire. In Proceedings of the 3rd Internatinoal Symposium on Connections between Steel and Concrete ConSC, Stuttgart, Germany, 27–29 September 2017.
26. *NF EN 12390-3, Essai pour béton durci—Partie 3: Résistance à la Compression des Éprouvettes*; Afnor Editions: Saint-Denis, France, 2019.
27. *Norme NF EN 12390-6 Essai Pour Béton Durci. Partie 6: Résistance en Traction par Fendage d'Éprouvettes*; Afnor Editions: Saint-Denis, France, 2012.
28. *NF EN 12390-13, Essai pour béton durci—Partie 13: Détermination du Module Sécant D'élasticité en Compression*; Afnor Editions: Saint-Denis, France, 2021.
29. Rilem TC 162-TDF: Test and Design Methods for Steel Fibre Reinforced Concrete. Available online: https://www.rilem.net/images/publis/1384.pdf (accessed on 26 January 2021).
30. EOTA TR048. *Details of Tests for Post-Installed Fasteners in Concrete*; EOTA: Ennepetal, Germany, 2016.
31. Petty, S.E. *Forensic Engineering: Damage Assessments for Residential and Commercial Structures*; CRC Press: Boca Raton, FL, USA, 2017; ISBN 978-1-4398-9974-8.